

RESEARCH ARTICLE

Diagnostic utility of plasma p-tau217 differs by Alzheimer's disease tau-based subtypes

Seyed Hani Hojjati¹  | Tracy A. Butler¹ | Seyed Javad Moosania Zare² | Ali Reihanian³ | Mohammad Khalafi¹ | Nancy Foldi¹ | Sudhin Shah¹ | Hasan Jafari³ | Yi Li¹ | Liangdong Zhou¹ | William Dartora¹ | Krista Wartchow¹ | Laura Beth J. McIntire¹ | Gloria C. Chiang¹ | for the Alzheimer's Disease Neuroimaging Initiative

¹Department of Radiology, Brain Health Imaging Institute, Weill Cornell Medicine, New York, New York, USA

²Department of Electrical Engineering, Babol Noshirvani University of Technology, Babol, Iran

³Department of Computer Engineering, Arak University, Arak, Iran

Correspondence

Seyed Hani Hojjati, Weill Cornell Medicine,
Department of Radiology, Brain Health
Imaging Institute, 407 East 61st Street, Room
RR-204, New York, NY 10065.
Email: shh4006@med.cornell.edu

[†] Data used in preparation of this article were obtained from the Alzheimer's Disease Neuroimaging Initiative (ADNI) database (adni.loni.usc.edu). As such, the investigators within the ADNI contributed to the design and implementation of ADNI and/or provided data but did not participate in analysis or writing of this report. A complete listing of ADNI investigators can be found at: http://adni.loni.usc.edu/wp-content/uploads/how_to_apply/ADNI_Acknowledgement_List.pdf

Funding information

the Alzheimer's Disease Neuroimaging Initiative (ADNI); National Institutes of Health, Grant/Award Number: U01 AG024904; ADNI Department of Defense award, Grant/Award Number: W81XWH-12-2-0012; National Institute on Aging; National Institute of Biomedical Imaging and Bioengineering; AbbVie; Alzheimer's Association; Alzheimer's Drug Discovery Foundation; Araclon Biotech; BioClinica, Inc.; Biogen; Bristol-Myers Squibb

Abstract

Introduction: Blood-based biomarkers, most notably plasma phosphorylated tau (p-tau)217, have transformed the diagnostic landscape of Alzheimer's disease (AD).

Methods: We applied an unsupervised machine learning approach to tau positron emission tomography (PET) imaging in 606 participants (age 73.95 ± 7.72 ; 309 female) to identify AD subtypes. Within each subtype, we evaluated plasma p-tau217 levels, their association with regional tau PET uptake, differences between cognitively unimpaired (CU) and cognitively impaired (CI) individuals, and relationships to cognitive performance.

Results: Four subtypes were identified: limbic, medial temporal lobe (MTL) sparing, posterior, and lateral temporal (l temporal). Plasma p-tau217 was elevated in CI versus CU in limbic, posterior, and l temporal subtypes and strongly associated with tau deposition and cognitive performance. In the MTL-sparing subtype, p-tau217 showed a significant association with tau but no elevation in CI and no relationship to cognition.

Discussion: These findings indicate that p-tau217's diagnostic utility varies across AD subtypes, reflecting distinct biological mechanisms not captured by current blood biomarkers.

KEYWORDS

Alzheimer's disease, atypical Alzheimer's disease, blood biomarker, phosphorylated tau217, tau positron emission tomography

Company; CereSpir, Inc.; Cogstate; Elan Pharmaceuticals, Inc.; Eli Lilly and Company; Eurolimmun; F. Hoffmann-La Roche Ltd and its affiliated company Genentech, Inc.; Fujirebio; GE Healthcare; IXICO Ltd.; Janssen Alzheimer Immunotherapy Research & Development, LLC; Johnson & Johnson Pharmaceutical Research & Development LLC; Lumosity; Lundbeck; Merck & Co., Inc.; Meso Scale Diagnostics, LLC; NeuroRx Research; Neurotrack Technologies; Novartis Pharmaceuticals Corporation; Pfizer Inc.; Piramal Imaging; Servier; Takeda Pharmaceutical Company; Transition Therapeutics; Canadian Institutes of Health Research; Alzheimer's Therapeutic Research Institute; University of Southern California

Highlights

- Plasma phosphorylated tau (p-tau)217 differentiated cognitively unimpaired from impaired individuals in most subtypes, with the notable limitation of the medial temporal lobe (MTL)-sparing group.
- P-tau217 level was linked to regional tau accumulation as measured by tau positron emission tomography, across all subtypes.
- The MTL-sparing subtype appeared to be unique, as p-tau217 was not elevated in cognitively impaired individuals, and there was no clear relationship between p-tau217 levels and cognitive performance.

1 | INTRODUCTION

Alzheimer's disease (AD) is a common neurodegenerative disorder characterized by a persistent and irreversible decline across multiple cognitive domains.^{1,2} Amyloid beta ($A\beta$) plaques and neurofibrillary tau tangles are two primary pathological hallmarks of AD that can be assessed at the regional and voxel-wise level in the brain using positron emission tomography (PET).³⁻⁵ Specifically, $A\beta$ has classically been considered a key driver of AD,^{1,6-8} although tau pathology has shown a closer association with brain atrophy⁹ and domain-specific cognitive decline.¹⁰⁻¹² Although PET imaging remains a powerful tool for assessing AD pathology,^{3,13-16} it is expensive and not widely accessible. Blood-based phosphorylated tau (p-tau)217 has demonstrated robust diagnostic performance in detecting AD pathology across the disease continuum, with higher accuracy in cognitively impaired individuals.¹⁷⁻²⁰

Most of the previous studies on p-tau217 have been conducted on cognitively unimpaired, mild cognitive impairment (MCI), and dementia cohorts broken down by $A\beta$ and/or tau status.^{18,21,22} In contrast to amnestic or typical AD, which is characterized by progressive memory loss, associated with abnormal $A\beta$ levels,^{23,24} and accompanied by a predictable spread of tau pathology,^{25,26} a significant subset of patients presents with atypical variants of AD that are more difficult to detect in the early stages of the disease. Atypical variants are particularly common in early-onset AD but also account for $\approx 6\%$ of late-onset cases.^{27,28} These individuals experience subtle impairments in language, visual processing, behavior, or executive function, along with asymmetric and atypical patterns of tau deposition, brain atrophy, and metabolism.²³ Because these atypical forms may arise earlier in life and do not follow the well-established tau, $A\beta$, and atrophy patterns seen in amnestic AD, they are more likely to be misdiagnosed or face delays in recognition, complicating treatment and resulting in increased mortality.²⁹

Previous studies have demonstrated that p-tau species have been shown to be associated with both amyloid plaques and tau tangles.^{30,31} Although p-tau 217 has helped improve the early detection of AD, we still know very little about accuracy in individuals with atypical forms of the disease, which can occur at younger ages and be more difficult

to diagnose clinically. Therefore, several important questions remain: Can plasma p-tau217 detect tau accumulation in individuals with atypical AD? Can it track regional tau deposition and cognitive decline in atypical AD? How well does it differentiate between cognitively unimpaired (CU) and cognitively impaired (CI) individuals with atypical tau patterns?

We hypothesize that the diagnostic utility of p-tau217 may vary across atypical presentations of AD due to distinct biological mechanisms of AD pathogenesis. To test our hypotheses, we first used an unsupervised machine learning technique to classify AD phenotypes by their tau deposition patterns on PET and then assessed how well plasma p-tau217 can detect AD pathology in each subtype.

2 | METHODS

2.1 | Participants

Our analysis included 686 cross-sectional participants from the Alzheimer's Disease Neuroimaging Initiative (ADNI) database (adni.loni.usc.edu) who had undergone tau PET, $A\beta$ PET imaging, p-tau217 blood biomarker, and cognitive assessments. We used 80 CU participants (age 65.35 ± 3.22 years; 50 females) as normative participants (all < 70 years old, apolipoprotein E [APOE] ε4-negative, and $A\beta$ -negative) to generate Z scores for each tau region of interest (ROI), which were used as standardized inputs for the unsupervised machine learning model. Finally, 606 remaining participants (age 73.95 ± 7.72 years; 309 females) were used as input for the unsupervised machine learning model, comprising 328 CU individuals and 278 CI patients diagnosed with either MCI or AD.

2.2 | Imaging and plasma data

We used preprocessed AV1451 tau PET data from the ADNI dataset as predictors using the machine learning technique. Standardized uptake value ratios (SUVRs) were extracted from 10 ROIs, including the bilateral frontal, occipital, parietal, temporal, and medial temporal lobe

(MTL). Notably, the temporal region is distinct from the MTL and targets the lateral temporal lobe regions (e.g., inferior and middle temporal gyri). These SUVR values were used to construct the tau dataset as the input to the method. To assess amyloid PET burden, we used the Centiloid measure available in the ADNI dataset and classified participants as A β negative or A β positive using a threshold of 18.^{32,33} For the blood biomarker, plasma p-tau217 levels (pg/mL) were measured in all participants using the fully automated Fujirebio LUMIPULSE G1200 platform.

2.3 | Cognitive assessments

ADNI used six cognitive assessment tests to capture different aspects of cognitive functioning across subtypes of AD: the Mini-Mental State Examination (MMSE), Clinical Dementia Rating Sum of Boxes (CDR-SB), Alzheimer's Disease Assessment Scale (ADAS), Wechsler Memory Scale Logical Memory, category fluency, and Trail Making Test Part B.

2.4 | Subtype and stage inference

We used the subtype and stage inference (SuStain), which is an unsupervised machine learning technique to map distinct stages of tau pathology and disease severity.^{34,35} Each region's tau progression was modeled using an age-adjusted linear Z score trajectory, approximated by a piecewise linear function.³⁵ Measurement noise was assumed to be constant over time and was estimated from a normative cohort of CU individuals. The normative CU individuals were participants under the age of 70, APOE ϵ 4 negative, and A β negative. SuStain determines the likelihood that an individual belongs to a particular stage of each subtype, then assigns them to the subtype and stage with the highest probability. Stages range from 0 to 30, with individuals who do not show abnormal tau in any brain region labeled as stage 0 and assigned to the no-tau group. We fitted SuStain following the procedures in³⁵ and used stratified 10-fold cross-validation to guide model selection and quantify uncertainty. For each fold, we trained SuStain on 90% of the data and evaluated the held-out 10% using the out-of-sample log likelihood; model selection across one to six subtypes was done by comparing the cross-validation information criterion (CVIC) and choosing the model with the best out-of-sample likelihood. Each candidate model was initialized hierarchically and uncertainty in event sequences and subject assignments was explored with 1,000,000 Markov chain Monte Carlo (MCMC) sampling. Both CVIC and log likelihood showed that model fit improved with increasing subtypes up to four, after which gains plateaued, indicating four subtypes as optimal.

2.5 | Statistical analyses

All statistical analyses were performed using Python. We assessed the normality of each variable distribution using the Shapiro-Wilk test to determine whether to apply parametric (e.g., t tests, Tukey hon-

RESEARCH IN CONTEXT

- Systematic Review:** Tau aggregation is a defining feature of neurodegenerative disorders, particularly Alzheimer's disease (AD). Recent progress in blood-based biomarkers has created new opportunities for monitoring AD pathology and progression. Among these, plasma phosphorylated tau (p-tau)217 has shown high diagnostic accuracy in detecting early AD pathology. However, most prior investigations have emphasized typical, amnestic forms of AD, while a substantial proportion of patients present with atypical variants characterized by early deficits in language, visuospatial processing, behavior, or executive function, and divergent patterns of tau deposition, atrophy, and metabolism. In this study, we investigated the diagnostic performance of plasma p-tau217 across these atypical presentations. We applied unsupervised machine-learning approaches to classify AD phenotypes based on tau positron emission tomography (PET) patterns and then evaluated the performance of plasma p-tau217 within each subtype.
- Interpretation:** Plasma p-tau217 was a robust discriminator of cognitively unimpaired versus cognitively impaired individuals, particularly within limbic and posterior-predominant subtypes, in which elevations were most pronounced. In contrast, diagnostic utility was limited in the medial temporal lobe (MTL)-sparing subtype. The p-tau217 level was linked to regional tau accumulation as measured by tau PET across all subtypes. The MTL-sparing subtype appeared distinct, as p-tau217 levels did not meaningfully relate to cognition, underscoring potential biological mechanisms not captured by current plasma measures.
- Future Directions:** Our findings support the utility of plasma p-tau217 for biological and clinical subtyping in AD, particularly for limbic and posterior tau PET-defined phenotypes, while highlighting limitations in MTL-sparing presentations. The distinct biomarker and clinical profile of MTL-sparing AD points to a potentially different disease trajectory or an earlier stage of pathology, meriting further investigation in future studies. Moreover, longitudinal investigations are needed to validate these patterns and clarify their temporal evolution.

estly significant difference [HSD], analysis of variance [ANOVA]) or non-parametric tests (e.g., Mann-Whitney U, Kruskal-Wallis). Notably, most of our statistical analyses used non-parametric tests. We used a two-sided 5% significance level for all tests, and P values were adjusted for multiple comparisons using the false discovery rate method (Benjamini-Hochberg).

2.5.1 | AD subtype characteristics

Demographic variables were compared across groups using Kruskal-Wallis and ANOVA, for continuous variables (e.g., age), and chi-squared tests for categorical variables (e.g., sex). We compared the pairwise difference between ROIs across all subtypes.

2.5.2 | Association between p-tau217 and regional tau deposition on PET (Z scored) within each AD subtype

We examined the association between p-tau217 levels and regional tau PET deposition levels (Z scores) across 10 ROIs (including bilateral frontal, occipital, parietal, temporal, and MTL) within each subtype. To assess this relationship, we conducted multiple linear regression analyses, adjusting for age and sex.

2.5.3 | Association between p-tau217 and the presence of cognitive impairment within each AD subtype

To compare plasma p-tau217 levels across subtypes, we first examined differences among the identified subtypes. To further evaluate the sensitivity of p-tau217 within each AD subtype, we conducted subgroup analyses based on the presence of cognitive impairment (CU versus CI).

2.5.4 | Association between p-tau217 and cognitive performance within each AD subtype

Finally, we explored how plasma p-tau217 levels relate to cognitive assessments within each subtype. We performed separate multiple regression analyses for each cognitive measure (ADAS, MMSE, CDR-SB, logical memory, category fluency, and Trail Making Test), adjusting for age and sex as covariates.

3 | RESULTS

3.1 | AD subtype characteristics

SuStain identified five distinct subtypes of AD based on patterns of tau deposition: one group with no detectable tau deposition (stage 0) and four AD subtypes (limbic, MTL sparing, posterior, and lateral temporal [l temporal]). Table 1 presents the demographic, clinical, and cognitive characteristics of these groups. There were significant ($P < 0.0063$) differences among the four subtypes in terms of age, sex, clinical diagnosis (CU versus CI), regional tau SUVR, and cognitive performance (e.g., ADAS, MMSE, and CDR-SB). Notably, the Centiloid levels and A β positivity were not significantly different across the four tau-positive subtypes ($P > 0.43$).

Figure 1A–D illustrates comparisons of average regional tau PET Z scores among the four subtypes. The limbic subtype showed high tau levels in the bilateral MTL and temporal regions (Z score > 3.7) and lowest tau levels in the bilateral occipital regions (Z score < 0.80). The MTL-sparing subtype had very low tau levels in bilateral MTL (Z score < 0.1) and temporal (Z score < 0.96), but relatively high tau in the left (Z score = 2) and right occipital (Z score = 1.74) regions. The posterior subtype showed elevated tau in bilateral occipital, parietal, and temporal regions (Z score > 3.71) and low tau levels in bilateral frontal (Z score < 1.41). The l temporal subtype had high tau in bilateral parietal, temporal (Z score > 2.89), and then frontal (Z score > 2.61), and lower tau levels in bilateral occipital (Z score < 1.30) and MTL (Z score < 1.70).

Figure S1A–E in the supporting information shows pairwise comparisons of bilateral tau deposition (Z scored) across the four subtypes. The l temporal subtype had the highest tau in the frontal lobe ($P < 0.0001$), while the posterior subtype had the highest occipital tau ($P < 0.0001$). The MTL-sparing subtype showed elevated occipital tau relative to the limbic subtype ($P < 0.0001$) and l temporal ($P < 0.001$) subtypes, while showing the lowest MTL and temporal lobe tau ($P < 0.0001$). Finally, the limbic subtype showed the highest MTL tau ($P < 0.0001$).

3.2 | Association between p-tau217 and regional tau deposition within each AD subtype

To examine the relationship between plasma p-tau217 levels and regional tau deposition (Zscored), we conducted multiple linear regression analyses within each AD subtype, controlling for age and sex. Results are presented in Figure 2A–J. In the limbic subtype, p-tau217 levels were significantly associated with tau deposition in all 10 ROIs except the left occipital region, with the strongest association observed in the left parietal region ($t = 7.64$, adjusted $P = 1.09e-11$, $r = 0.532$). The MTL-sparing subtype showed no significant associations in the left frontal and right MTL regions and strong associations in bilateral parietal and left temporal regions ($t > 3.29$, adjusted $P < 0.00218$, $r > 0.395$) and then left occipital ($t = 2.56$, adjusted $P = 0.0116$, $r = 0.346$). In contrast, the posterior subtype exhibited robust associations between p-tau217 and tau deposition across all 10 ROIs ($t > 5.73$, adjusted $P < 4.64e-7$, $r > 0.558$), indicating that plasma p-tau217 robustly reflected tau pathology in this subtype. Finally, in the l temporal subtype, the statistical relationship was generally weaker than in the posterior subtype but stronger than in both the limbic and MTL-sparing subtypes, with adjusted P values between 0.028 and 1.53e-14.

We repeated the analyses in A β -positive individuals (Figure S2A–J in supporting information), and the results were largely consistent. The limbic subtype showed significant p-tau217 associations in parietal, temporal, and MTL region ($t > 3.01$, adjusted $P < 0.00558$, $r > 0.352$). The MTL-sparing subtype showed associations across most ROIs ($t > 2.56$, adjusted $P < 0.0206$, $r > 0.45$), except right frontal, right occipital, and bilateral MTL. Posterior and l temporal subtypes showed strong associations in all regions.

TABLE 1 Participant demographics.

	No tau	Limbic (subtype 1)	MTL sparing (subtype 2)	Posterior (subtype 3)	L temporal (subtype 4)	Statistics ^a
Number of individuals	226	155	63	77	85	
Age (mean \pm SD)	70.76 \pm 6.77	74.55 \pm 7.64	79.43 \pm 6.29	77.81 \pm 7.31	73.08 \pm 7.46	P = 1.11e-6 ^b
Sex (male /female)	117 / 109	88 / 67	21 / 42	37 / 40	34 / 51	P = 0.0063 ^c
Number of CU/CI	162 / 64	44 / 111	44 / 19	24 / 53	54 / 31	P = 5.46e-11 ^c
A β negative/A β positive	178 / 48	56 / 99	28 / 35	30 / 47	39 / 46	P = 0.43 ^d
Centiloid value (mean \pm SD)	10 \pm 30.26	44.28 \pm 54.43	44.25 \pm 59.80	51.40 \pm 58.15	40.89 \pm 44.39	P = 0.51 ^d
Frontal tau SUVR (mean \pm SD)	1.42 \pm 0.26	1.56 \pm 0.18	1.57 \pm 0.10	1.59 \pm 0.24	1.74 \pm 0.33	P = 5.24e-22 ^c
Occipital tau SUVR (mean \pm SD)	1.43 \pm 0.52	1.51 \pm 0.14	1.64 \pm 0.16	2.15 \pm 0.69	1.56 \pm 0.19	P = 1.09e-31 ^c
Parietal tau SUVR (mean \pm SD)	1.45 \pm 0.52	1.60 \pm 0.24	1.61 \pm 0.14	1.84 \pm 0.47	1.78 \pm 0.44	P = 9.50e-14 ^c
Lateral temporal tau SUVR (mean \pm SD)	1.39 \pm 0.26	1.8 \pm 0.38	1.51 \pm 0.13	1.88 \pm 0.56	1.77 \pm 0.46	P = 3.35e-33 ^c
MTL tau SUVR (mean \pm SD)	1.34 \pm 0.21	2.10 \pm 0.49	1.46 \pm 0.18	1.95 \pm 0.69	1.71 \pm 0.37	P = 1.50e-63 ^c
CDR-SB score (mean \pm SD)	0.55 \pm 1.25	1.42 \pm 2.40	0.47 \pm 1.24	2.44 \pm 3.10	0.94 \pm 2.65	P = 1.42e-12 ^d
ADAS score (mean \pm SD)	9.87 \pm 6.39	17.40 \pm 9.75	10.22 \pm 6.81	18.89 \pm 10.39	12.55 \pm 9.04	P = 5.28e-10 ^d
MMSE score (mean \pm SD)	28.58 \pm 1.85	26.91 \pm 3.63	28.73 \pm 2.06	26.25 \pm 3.58	26.96 \pm 3.38	P = 7.52e-8 ^d
Logical memory (mean \pm SD)	11.99 \pm 4.28	7.07 \pm 5.64	12.65 \pm 4.80	7.04 \pm 5.74	11.38 \pm 5.30	P = 6.45e-13 ^d
Category fluency (mean \pm SD)	21 \pm 5.61	17.75 \pm 6.10	19.17 \pm 4.57	16.59 \pm 5.79	19.73 \pm 6.10	P = 0.0032 ^b
Trail Making B (mean \pm SD)	81.04 \pm 48.34	103.46 \pm 61.04	87.80 \pm 38.15	137.62 \pm 79.48	92.5 \pm 54.10	P = 9.46e-5 ^d

Abbreviations: A β , amyloid beta; ADAS, Alzheimer's Disease Assessment Scale; CDR-SB, Clinical Dementia Rating Sum of Boxes; CI, cognitive impaired; CU, cognitive unimpaired; MMSE, Mini-Mental State Examination; MTL, medial temporal lobe; SD, standard deviation; SUVR, standardized uptake value ratio.

^aStatistical test has been applied across four subtypes (limbic, MTL sparing, posterior, lateral temporal).

^bChi-squared.

^cAnalysis of variance (ANOVA).

^dKruskal-Wallis.

3.3 | Comparisons of p-tau217 across AD subtypes

In Figure 3A, we compared p-tau217 levels across the four subtypes. The results showed that both the limbic and posterior subtypes had significantly higher p-tau217 levels compared to the MTL-sparing subtype (mean difference [Δ] $>$ 0.14, adjusted P $<$ 4e-5). Also, the posterior subtype had significantly higher p-tau217 level than the I temporal subtype (Δ $>$ 0.1, adjusted P $<$ 0.0292). Next, to assess the clinical relevance of p-tau217, we examined its levels in CU versus CI individuals within each subtype (Figure 3B). In all subtypes except MTL sparing, CI participants had significantly higher p-tau217 levels compared to CU (Δ $>$ 0.19, adjusted P value $<$ 0.000606). Post hoc power analysis based on the effect size from the posterior subtype ($d \approx 1.20$, power $\approx 99\%$) indicates that the non-significant association in the MTL-sparing subtype is unlikely due to limited sample size.

In A β -positive individuals (Figure S3A–B in supporting information), all findings were replicated. Limbic and posterior subtypes showed higher p-tau217 than MTL-sparing ($\Delta > 0.12$, adjusted P $<$ 0.0115) and I temporal ($\Delta > 0.09$, adjusted P $<$ 0.0114). Within subtypes, CI participants had higher p-tau217 than CU ($\Delta > 0.16$, adjusted P $<$ 0.0454), except in MTL sparing.

3.4 | Association between p-tau217 and cognitive performance within each AD subtype

To investigate how plasma p-tau217 levels relate to cognitive performance within each AD subtype, we conducted multiple linear regression analyses, controlling for age and sex. Results are illustrated in Figure 4A–F. As shown in Figure 4A, p-tau217 levels were strongly associated with MMSE scores in the limbic, posterior, and I temporal

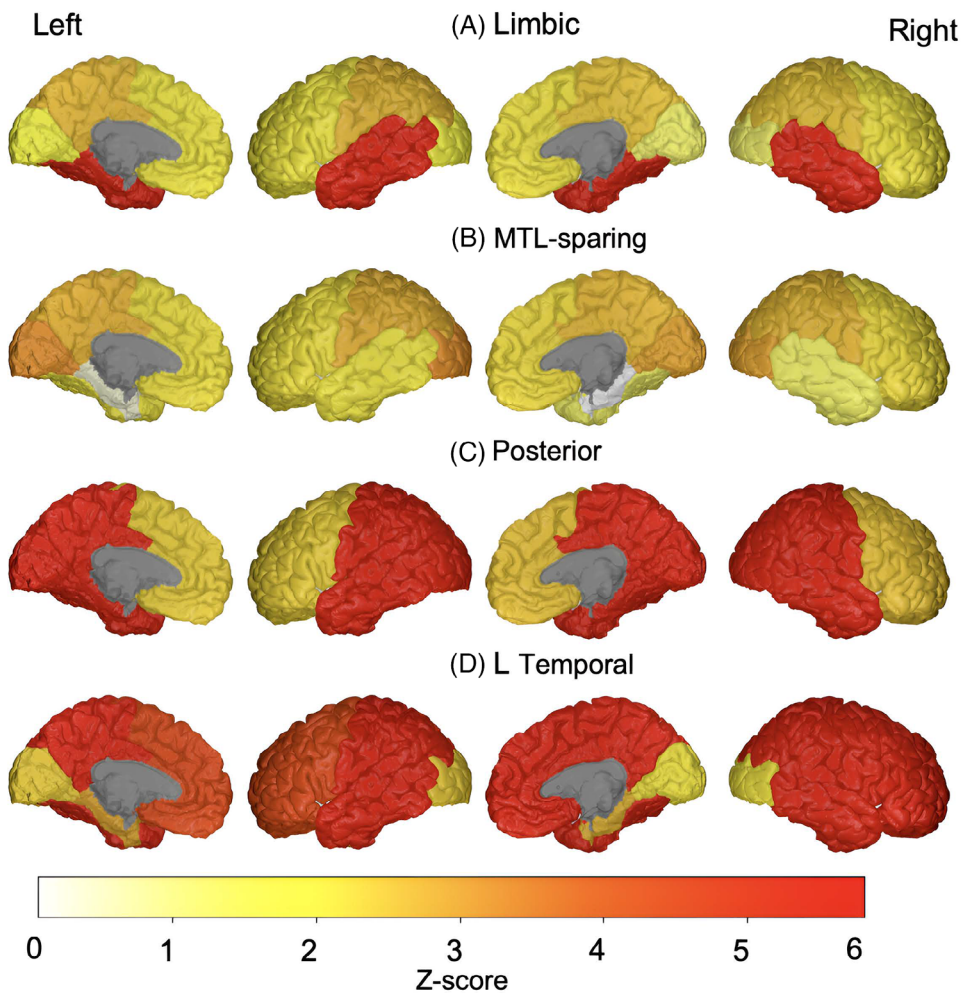


FIGURE 1 Comparisons of average regional tau levels (Z scores) in 10 ROIs (bilateral frontal, occipital, parietal, temporal, and MTL) across four subtypes: (A) limbic; (B) MTL sparing; (C) posterior; (D) I temporal. I temporal, lateral temporal; MTL, medial temporal lobe; ROI, region of interest

subtypes ($t < -4.85$, adjusted $P < 8.95\text{e-}6$, $r < -0.363$). No significant association was observed in the MTL-sparing subtype. Similarly, Figure 4B showed that CDR-SB scores were also strongly associated with p-tau217 levels in the limbic, posterior, and I temporal subtypes ($t > 3.78$, adjusted $P < 0.000422$, $r > 0.308$), again with no significant relationship in the MTL-sparing group. Figure 4C presented the ADAS results, for which strong associations persisted in the limbic, posterior, and I temporal subtypes ($t > 4.13$, adjusted $P < 8.31\text{e-}5$, $r > 0.321$). Again, no significant association was observed in the MTL-sparing subtype. In Figure 4D, logical memory scores showed strong negative associations with p-tau217 in the limbic, posterior, and I temporal subtypes ($t < -3.25$, adjusted $P < 0.00237$, $r < -0.356$). Figure 4E illustrates the associations of category fluency scores. Significant associations were observed in the limbic, posterior, and I temporal subtypes, with the posterior subtype showing a particularly robust association ($t = -5.18$, adjusted $P = 8.7\text{e-}6$, $r = -0.537$). Finally, Figure 4F showed results for the Trail Making Test, for which significant associations were observed in the limbic, posterior, and I temporal subtypes ($t > 2.17$, adjusted $P = 0.0425$, $r > 0.176$). There were no significant associations in the limbic and MTL-sparing subtypes.

In the MTL-sparing subtype, p-tau217 was not associated with cognition. To examine whether tau deposition itself was associated with cognitive performance in this subtype and address potential sample size limitations, we conducted multiple regression analyses between ADAS scores and tau deposition levels, controlling for age and sex. Regression analyses in Figure 5 showed that tau deposition in bilateral occipital, parietal, and temporal regions was significantly related to ADAS scores ($t > 2.57$, adjusted $P < 0.0219$, $r > 0.266$; Figure 5), suggesting regional tau (but not p-tau217) captured cognitive decline in this subtype.

4 | DISCUSSION

In this study, we investigated how plasma p-tau217 levels relate to AD subtypes as categorized by tau deposition patterns and their clinical significance. Our findings offer several important insights into the potential and limitations of p-tau217 as a biomarker in AD subtypes. First, p-tau217 emerged as a strong marker for distinguishing CU from CI individuals, particularly in the limbic and posterior subtypes

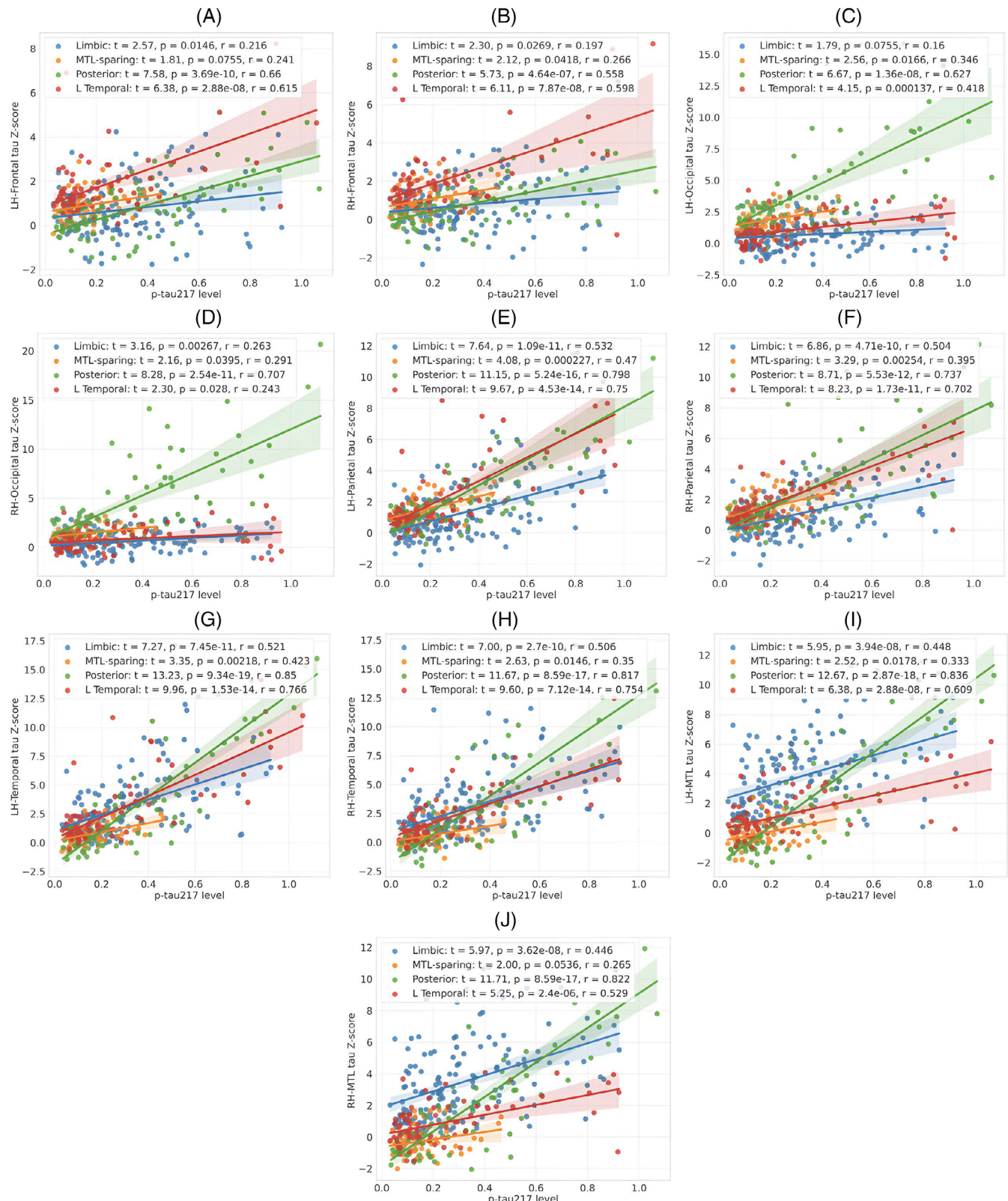


FIGURE 2 Associations between p-tau217 and tau levels (Z score) in 10 ROIs. (A) LH-Frontal; (B) RH-Frontal; (C) LH-Occipital; (D) RH-Occipital; (E) LH-Parietal; (F) RH-Parietal; (G) LH-Temporal; (H) RH-Temporal; (I) LH-MTL; (J) RH-MTL. All P values were adjusted for multiple comparison corrections. LH, left hemisphere; I temporal, lateral temporal; MTL, medial temporal lobe; p-tau, phosphorylated tau; RH, right hemisphere; ROI, region of interest

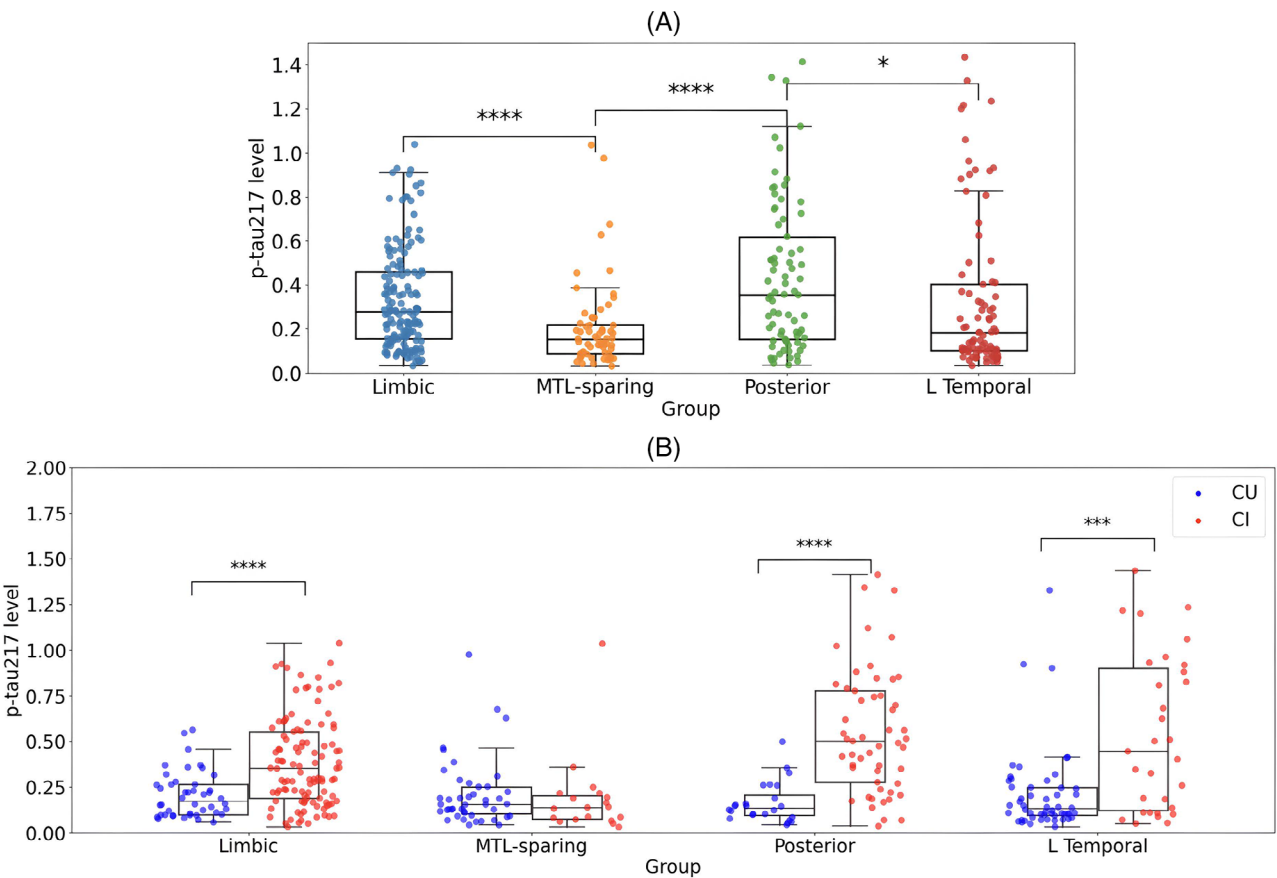


FIGURE 3 A, Comparison of p-tau217 levels in four subtypes (limbic, MTL sparing, posterior, and L temporal) using both CU and CI individuals. B, Comparison of p-tau217 levels in four subtypes (limbic, MTL sparing, posterior, and L temporal) across CU and CI. Only associations that remained significant after adjusting P values for multiple comparisons are reported. * $P < 0.05$, ** $P < 0.01$, *** $P < 0.001$, and **** $P < 0.0001$. CI, cognitively impaired; CU, cognitively unimpaired; L temporal, lateral temporal; MTL, medial temporal lobe; p-tau, phosphorylated tau

with robust elevations. In contrast, its diagnostic utility was lower in the MTL-sparing subtype. Second, the p-tau217 level was linked to regional tau accumulation as measured by tau PET across all subtypes. Third, the MTL-sparing subtype appeared to be unique, as p-tau217 was not elevated in CI individuals, and there was no clear relationship between p-tau217 levels and cognitive performance. This points to the possibility that tau in this subtype may accumulate through different biological mechanisms not captured by current plasma biomarkers or indicate an earlier disease stage.

Our findings contribute to the growing body of evidence supporting plasma p-tau217 as a promising biomarker for AD. This is particularly concordant for the limbic subtype, which closely follows the typical amnestic presentation.^{34,36–40} Although we considered the limbic subtype as a proxy for typical AD that follows Braak staging,⁴¹ prior studies have contrasted the limbic-predominant variant with the typical form, which often exhibits tau pathology in both the MTL and neocortex.^{42,43} Consistent with previous studies showing that p-tau217 can reliably identify CU individuals who are A β - and tau PET positive, we observed elevated plasma p-tau217 levels in CI individuals in the limbic subtype.^{38,39} We also showed that these elevations strongly correlated with regional tau PET uptake and cognitive performance.

Similarly, in the posterior subtype with the presence of tau in occipital and parietal lobes, p-tau217 levels were also elevated in CI individuals and showed robust associations with both regional tau and cognitive performance. The posterior subtype closely resembles posterior cortical atrophy, the visual variant of AD, which is characterized by greater occipital hypometabolism and tau deposition.²⁷ The relationship between p-tau217, tau accumulation, and cognitive impairment appeared even stronger in this group compared to the other subtypes. This suggests that the posterior subtype may represent a more aggressive form of AD,⁴³ for which p-tau217 could be particularly effective as a robust biomarker for this subtype of AD. Prior research supports the idea that greater tau accumulation in neocortical regions, compared to the MTL, is more predictive of future cognitive decline.⁴⁴ Moreover, the posterior subtype is commonly seen in early-onset AD, and several studies have indicated that early-onset cases may follow a more aggressive clinical trajectory.^{45,46} However, a slower clinical progression in this subtype has been reported despite its neocortical tau dominance.³⁴ The L temporal subtype is characterized by temporal, parietal, and frontal lobe tau predominance. It closely follows the limbic and posterior subtypes in terms of p-tau217 elevation and in the strength of its association with tau deposition

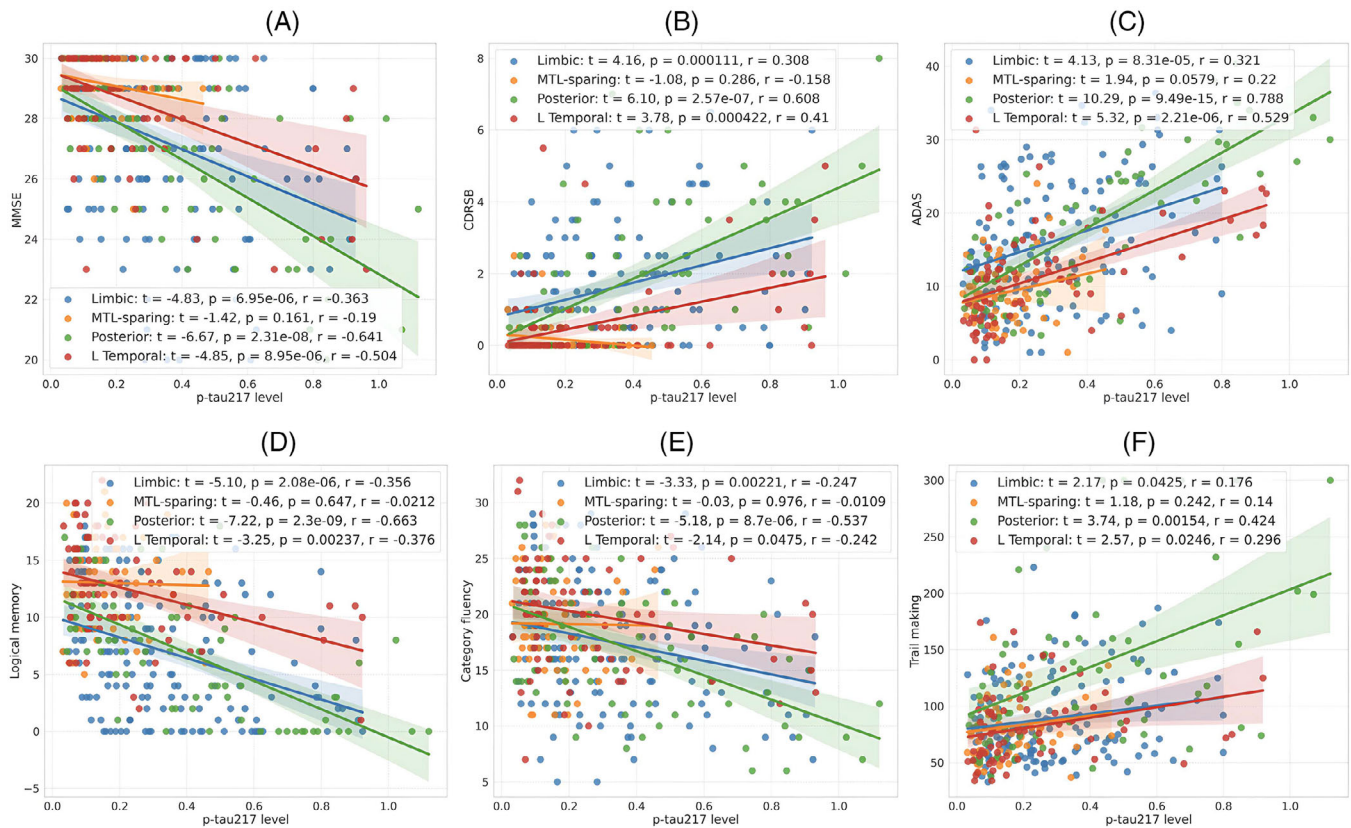


FIGURE 4 Associations between p-tau217 levels and cognitive performance: (A) MMSE; (B) CDR-SB; (C) ADAS; (D) Logical memory; (E) Category fluency; (F) Trail Making. All P values were adjusted for multiple comparison corrections. ADAS, Alzheimer's Disease Assessment Scale; CDR-SB, Clinical Dementia Rating Sum of Boxes; MMSE, Mini-Mental State Examination

and cognitive performance. However, this subtype has less overall elevation compared to limbic and posterior subtypes.

The MTL-sparing subtype emerged as a potentially biologically distinct subtype. Unlike the other subtypes, this group showed no significant differences in p-tau217 levels between CI and CU individuals. Moreover, there was no association with cognitive performance. Reports on the MTL-sparing subtype (also referred to as hippocampal sparing) have mainly linked it to younger age, earlier disease onset, and a more aggressive clinical course.⁴⁷ In our cohort, the MTL-sparing subgroup was slightly older and showed better cognitive performance than the other subtypes, lower Centiloid levels, lower cortical tau levels, and minimal MTL tau accumulation.

To our knowledge, this is the first study to examine the association between the blood-based p-tau217 biomarker and atypical variants of AD. A previous post mortem study⁴⁸ examined plasma p-tau217 levels across individuals with various tauopathies, and they showed that the elevation of the p-tau217 is potentially higher in A β -positive subjects and selective to AD pathologies. They also reported that individuals with an intermediate likelihood of AD with a similar level of A β pathology did not show significant differences from other groups, which also suggests that the presence of A β alone may not be sufficient to drive a significant elevation in p-tau217 biomarker. This raises the possibility that certain atypical patterns, such as MTL-sparing tau deposition, may reflect alternative disease

pathways that are not necessarily driven by established A β -related AD mechanisms.

This aligns with our previous works, which demonstrated that neocortical tau pathology may emerge independently of A β ²⁴, and neocortical tau patterns were not significantly associated with A β in preclinical stages.¹⁶ An alternative explanation for our findings is that the MTL-sparing subtype, which showed pronounced occipital tau involvement, may reflect a distinct neuropathological process even not related to AD. Occipital tau accumulation is a hallmark feature of dementia with Lewy bodies (DLB)⁴⁹ and is often used to distinguish it from typical AD. Therefore, the tau pattern observed in the MTL-sparing subtype may point to underlying α -synuclein pathology or even a mixed pathology that includes features of both AD and DLB.⁵⁰

This study has several limitations that may need to be addressed in future research. First, atypical AD variants are more common in young-onset cases and comprise only $\approx 6\%$ of late-onset cases,^{27,28} resulting in smaller atypical subtype individuals and potentially reduced statistical power, especially in subgroup analyses stratified by cognitive or A β status. Second, the cross-sectional design limits causal implications. Longitudinal studies in independent cohorts are needed to assess the temporal effects and predictive value of plasma p-tau217 across subtypes.

This work supports plasma p-tau217 as a valuable biomarker for AD subtyping, particularly limbic and posterior patterns, though less

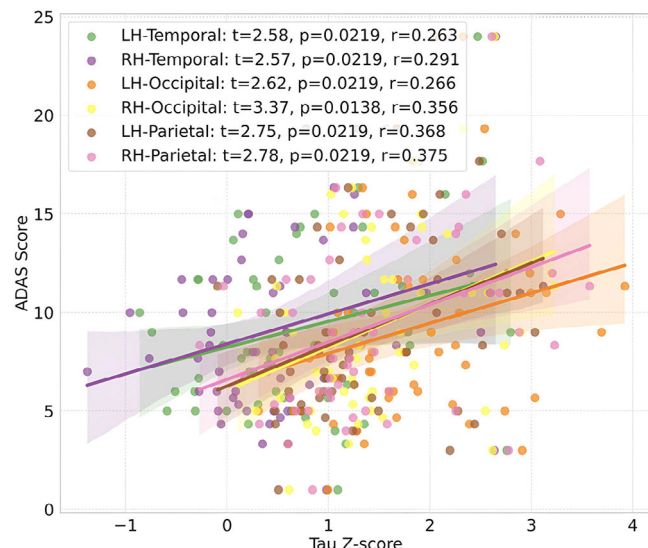


FIGURE 5 Associations between tau levels (Z score) in brain ROIs and ADAS score in MTL-sparing subtype. Only associations that remained significant after adjusting P values for multiple comparisons are reported. ADAS, Alzheimer's Disease Assessment Scale; MTL, medial temporal lobe; ROI, region of interest

effective in MTL sparing. The distinct profile of MTL sparing suggests a unique trajectory or earlier stage not captured by current plasma measures.

ACKNOWLEDGMENTS

Data collection and sharing for this project funded by the Alzheimer's Disease Neuroimaging Initiative (ADNI; National Institutes of Health Grant U01 AG024904) and DOD (ADNI Department of Defense award number W81XWH-12-2-0012). ADNI is funded by the National Institute on Aging, the National Institute of Biomedical Imaging and Bioengineering, and through generous contributions from the following: AbbVie; Alzheimer's Association; Alzheimer's Drug Discovery Foundation; Araclon Biotech; BioClinica, Inc.; Biogen; Bristol-Myers Squibb Company; CereSpir, Inc.; Cogstate; Eisai Inc.; Elan Pharmaceuticals, Inc.; Eli Lilly and Company; EuroImmun; F. Hoffmann-La Roche Ltd and its affiliated company Genentech, Inc.; Fujirebio; GE Healthcare; IXICO Ltd.; Janssen Alzheimer Immunotherapy Research & Development, LLC; Johnson & Johnson Pharmaceutical Research & Development LLC; Lumosity; Lundbeck; Merck & Co., Inc.; Meso Scale Diagnostics, LLC; NeuroRx Research; Neurotrack Technologies; Novartis Pharmaceuticals Corporation; Pfizer Inc.; Piramal Imaging; Servier; Takeda Pharmaceutical Company; and Transition Therapeutics. The Canadian Institutes of Health Research is providing funds to support ADNI clinical sites in Canada. Private sector contributions are facilitated by the Foundation for the National Institutes of Health (www.fnih.org). The grantee organization is the Northern California Institute for Research and Education, and the study is coordinated by the Alzheimer's Therapeutic Research Institute at the University of Southern California. ADNI data are disseminated by the Laboratory for Neuro Imaging at the University of Southern California.

CONFLICT OF INTEREST STATEMENT

The authors declare that the research was conducted in the absence of any commercial or financial relationships that could be construed as a potential conflict of interest. Author disclosures are available in the supporting information.

DATA AVAILABILITY STATEMENT

Publicly available datasets were analyzed in this study. This data can be found here: adni.loni.usc.edu.

ETHICS STATEMENT

As per Alzheimer's Disease Neuroimaging Initiative (ADNI) protocols, all procedures conducted in studies involving human participants adhered to ethical standards. The ADNI data collection was conducted after obtaining written informed consent from the participants. Further details can be found at adni.loni.usc.edu.

FUNDING STATEMENT

The author(s) declare that no financial support was received for the research, authorship, and/or publication of this article.

CONSENT STATEMENT

All human subjects provided informed consent according to the ADNI study protocol, approved by the institutional review boards of all participating sites.

ORCID

Seyed Hani Hojjati  <https://orcid.org/0000-0003-3900-9603>

REFERENCES

- Jagust W. Imaging the evolution and pathophysiology of Alzheimer disease. *Nat Rev Neurosci*. 2018;19(11):687-700. [10.1038/s41583-018-0067-3](https://doi.org/10.1038/s41583-018-0067-3)
- Hojjati SH, Babajani-Feremi A. Prediction and modeling of neuropsychological scores in Alzheimer's disease using multimodal neuroimaging data and artificial neural networks. *Front Comput Neurosci*. 2022;15:769982. [10.3389/fncom.2021.769982](https://doi.org/10.3389/fncom.2021.769982)
- Hojjati SH, Feiz F, Ozoria S, Razlighi QR. Topographical overlapping of the amyloid- β and tau pathologies in the default mode network predicts Alzheimer's disease with higher specificity. *J Alzheimers Dis*. 2021;83(1):407-421. [10.3233/JAD-210419](https://doi.org/10.3233/JAD-210419)
- Sintini I, Martin PR, Graff-Radford J, et al. Longitudinal tau-PET uptake and atrophy in atypical Alzheimer's disease. *Neuroimage Clin*. 2019;23:101823. [10.1016/j.nicl.2019.101823](https://doi.org/10.1016/j.nicl.2019.101823)
- Stancu IC, Vasconcelos B, Terwel D, Dewachter I. Models of β -amyloid induced Tau-pathology: the long and "folded" road to understand the mechanism. *Mol Neurodegener*. 2014;9:51. [10.1186/1750-1326-9-51](https://doi.org/10.1186/1750-1326-9-51)
- Vasconcelos B, Stancu I, Buist A, et al. Heterotypic seeding of Tau fibrillation by pre-aggregated Abeta provides potent seeds for prion-like seeding and propagation of Tau-pathology in vivo. *Acta Neuropathol*. 2016;131(4):549-569. [10.1007/s00401-015-1525-x](https://doi.org/10.1007/s00401-015-1525-x)
- Musiek ES, Holtzman DM. Origins of Alzheimer's Disease: reconciling CSF biomarker and neuropathology data regarding the temporal sequence of A-beta and tau involvement. *Curr Opin Neurobiol*. 2012;25(6):715-720. [10.1097/WCO.0b013e32835a30f4](https://doi.org/10.1097/WCO.0b013e32835a30f4)

8. Hardy JA, Higgins GA. Alzheimer's disease: the amyloid cascade hypothesis. *Science*. 1992;256(5054):184-185. [10.1126/science.1566067](https://doi.org/10.1126/science.1566067)
9. La Joie R, Visani AV, Baker SL, et al. Prospective longitudinal atrophy in Alzheimer's disease correlates with the intensity and topography of baseline tau-PET. *Sci Transl Med*. 2020;12(524):eaau5732. [10.1126/scitranslmed.aau5732](https://doi.org/10.1126/scitranslmed.aau5732)
10. Reitz C, Honig L, Vonsattel JP, Tang MX, Mayeux R. Memory performance is related to amyloid and tau pathology in the hippocampus. *J Neurol Neurosurg Psychiatry*. 2009;80(7):715-721. [10.1136/jnnp.2008.154146](https://doi.org/10.1136/jnnp.2008.154146)
11. Rani N, Alm KH, Corona-Long CA, et al. Tau PET burden in Brodmann areas 35 and 36 is associated with individual differences in cognition in non-demented older adults. *Front Aging Neurosci*. 2023;15:1272946. [10.3389/fnagi.2023.1272946](https://doi.org/10.3389/fnagi.2023.1272946)
12. Bejanin A, Schonhaut DR, La Joie R, et al. Tau pathology and neurodegeneration contribute to cognitive impairment in Alzheimer's disease. *Brain*. 2017;140(12):3286-3300. [10.1093/brain/awx243](https://doi.org/10.1093/brain/awx243)
13. Hojjati SH, Habeck C, Butler TA, et al. Early accumulation of A β and Tau is associated with increase in cortical thickness. *Alzheimer's & Dementia*. 2022;18(S5):e063715. [10.1002/alz.063715](https://doi.org/10.1002/alz.063715)
14. Hojjati SH, Butler TA, de Leon M, et al. Inter-network functional connectivity increases by beta-amyloid and may facilitate the early stage of tau accumulation. *Neurobiol Aging*. 2025;148:16-26. [10.1016/j.neurobiolaging.2025.01.005](https://doi.org/10.1016/j.neurobiolaging.2025.01.005)
15. Hani Hojjati S, Butler TA, Chiang GC, et al. Distinct and joint effects of low and high levels of A β and tau deposition on cortical thickness. *Neuroimage Clin*. 2023;38:103409. [10.1016/j.nicl.2023.103409](https://doi.org/10.1016/j.nicl.2023.103409)
16. Hojjati SH, Chiang GC, Butler TA, et al. Remote associations between tau and cortical amyloid- β are stage-dependent. *J Alzheimers Dis*. 2024;98(4):1467-1482. [10.3233/JAD-231362](https://doi.org/10.3233/JAD-231362)
17. Jack CR, Wiste HJ, Algeciras-Schimmele A, et al. Comparison of plasma biomarkers and amyloid PET for predicting memory decline in cognitively unimpaired individuals. *Alzheimer's and Dementia*. 2024;20(3):2143-2154. [10.1002/alz.13651](https://doi.org/10.1002/alz.13651)
18. Ossenkoppele R, Salvadó G, Janelidze S, et al. Plasma p-tau217 and tau-PET predict future cognitive decline among cognitively unimpaired individuals: implications for clinical trials. *Nat Aging*. 2025;5(5):883-896. [10.1038/s43587-025-00835-z](https://doi.org/10.1038/s43587-025-00835-z)
19. Khalafi M, Dartora WJ, McIntire LBJ, et al. Diagnostic accuracy of phosphorylated tau217 in detecting Alzheimer's disease pathology among cognitively impaired and unimpaired: a systematic review and meta-analysis. *Alzheimers Dement*. 2025;21(2):e14458. [10.1002/alz.14458](https://doi.org/10.1002/alz.14458). John Wiley and Sons Inc.[CrossRef]
20. Ashton NJ, Brum WS, Di Molfetta G, et al. Diagnostic accuracy of a plasma phosphorylated tau 217 immunoassay for Alzheimer disease pathology. *JAMA Neurol*. 2024;81(3):255-263. [10.1001/jamaneurol.2023.5319](https://doi.org/10.1001/jamaneurol.2023.5319)
21. Barthélémy NR, Salvadó G, Schindler SE, et al. Highly accurate blood test for Alzheimer's disease is similar or superior to clinical cerebrospinal fluid tests. *Nat Med*. 2024;30(4):1085-1095. [10.1038/s41591-024-02869-z](https://doi.org/10.1038/s41591-024-02869-z)
22. Pandey N, Yang Z, Cieza B, et al. Plasma phospho-tau217 as a predictive biomarker for Alzheimer's disease in a large south American cohort. *Alzheimers Res Ther*. 2025;17(1):1. [10.1186/s13195-024-01655-w](https://doi.org/10.1186/s13195-024-01655-w)
23. Graff-Radford J, et al. New insights into atypical Alzheimer's disease in the era of biomarkers. *Lancet Neurol*. 2021;20(3):222-234.. [https://doi.org/10.1016/S1474-4422\(20\)30440-3](https://doi.org/10.1016/S1474-4422(20)30440-3)
24. Hojjati SH, Chiang GC, Butler TA, et al. Heterogeneous tau deposition patterns in the preclinical stage link to domain-specific cognitive deficits. *Alzheimer's and Dementia*. 2025;21(5):e70153. [10.1002/alz.70153](https://doi.org/10.1002/alz.70153)
25. Braak H, Braak E. Staging of alzheimer's disease-related neurofibrillary changes. *Neurobiol Aging*. 1995;16(3):271-278. [10.1016/0197-4580\(95\)00021-6](https://doi.org/10.1016/0197-4580(95)00021-6)
26. Braak H, Alfafurri I, Arzberger T, Kretschmar H, Del Tredici K. Staging of Alzheimer disease-associated neurofibrillary pathology using paraffin sections and immunocytochemistry. *Acta Neuropathol*. 2006;112(4):389-404. [10.1007/s00401-006-0127-z](https://doi.org/10.1007/s00401-006-0127-z)
27. Whitwell JL. Atypical clinical variants of Alzheimer's disease: are they really atypical? *Front Neurosci*. 2024;18:1352822. [10.3389/fnins.2024.1352822](https://doi.org/10.3389/fnins.2024.1352822)
28. Mendez MF. Early-onset Alzheimer disease and its variants. *Continuum (Minneapolis Minn)*. 2019;25(1):34-51. [10.1212/CON.000000000000687](https://doi.org/10.1212/CON.000000000000687)
29. Bader I, Groot C, Van Der Flier WM, Pijnenburg YAL, Ossenkoppele R. Survival differences between individuals with typical and atypical phenotypes of Alzheimer disease. *Neurology*. 2025;104(10):e213603. [10.1212/WNL.000000000000213603](https://doi.org/10.1212/WNL.000000000000213603)
30. Salvadó G, Ossenkoppele R, Ashton NJ, et al. Specific associations between plasma biomarkers and postmortem amyloid plaque and tau tangle loads. *EMBO Mol Med*. 2023;15(5):e17123. [10.15252/emmm.202217123](https://doi.org/10.15252/emmm.202217123)
31. Mattsson-Carlsgren N, Janelidze S, Bateman RJ, et al. Soluble P-tau217 reflects amyloid and tau pathology and mediates the association of amyloid with tau. *EMBO Mol Med*. 2021;13(6):e14022. [10.15252/emmm.202114022](https://doi.org/10.15252/emmm.202114022)
32. Khalafi M, Hojjati SH, Wang XH, et al. Concordance between Centiloid quantification and visual interpretation of amyloid PET scans across the Alzheimer's disease continuum. *Am J Neuroradiol*. 2025;46(9):1884-1892. [10.3174/ajnr.A8743](https://doi.org/10.3174/ajnr.A8743). p. ajnr.A8743.[CrossRef]
33. Farrell ME, Jiang S, Schultz AP, et al. Defining the Lowest threshold for Amyloid-PET to predict future cognitive decline and amyloid accumulation. *Neurology*. 2021;96(4):e619-e631. [10.1212/WNL.00000000000011214](https://doi.org/10.1212/WNL.00000000000011214)
34. Vogel JW, Young AL, Oxtoby NP, et al. Four distinct trajectories of tau deposition identified in Alzheimer's disease. *Nat Med*. 2021;27(5):871-881. [10.1038/s41591-021-01309-6](https://doi.org/10.1038/s41591-021-01309-6)
35. Young AL, Marinescu RV, Oxtoby NP, et al. Uncovering the heterogeneity and temporal complexity of neurodegenerative diseases with subtype and stage inference. *Nat Commun*. 2018;9(1):4273. [10.1038/s41467-018-05892-0](https://doi.org/10.1038/s41467-018-05892-0)
36. Milà-Alomà M, Ashton NJ, Shekari M, et al. Plasma p-tau231 and p-tau217 as state markers of amyloid- β pathology in preclinical Alzheimer's disease. *Nat Med*. 2022;28(9):1797-1801. [10.1038/s41591-022-01925-w](https://doi.org/10.1038/s41591-022-01925-w)
37. Janelidze S, Palmqvist S, Leuzy A, et al. Detecting amyloid positivity in early Alzheimer's disease using combinations of plasma A β 42/A β 40 and p-tau. *Alzheimer's and Dementia*. 2022;18(2):283-293. [10.1002/alz.12395](https://doi.org/10.1002/alz.12395)
38. Mattsson-Carlsgren N, Janelidze S, Palmqvist S, et al. Longitudinal plasma p-tau217 is increased in early stages of Alzheimer's disease. *Brain*. 2021;143(11):3234-3241. [10.1093/BRAIN/AWAA286](https://doi.org/10.1093/BRAIN/AWAA286)
39. Lai R, Li B, Bishnoi R. P-tau217 as a reliable blood-based marker of Alzheimer's disease. *Biomedicines*. 2024;12(8):1836. [10.3390/biomedicines12081836](https://doi.org/10.3390/biomedicines12081836). Multidisciplinary Digital Publishing Institute (MDPI).[CrossRef]
40. Therriault J, Ashton NJ, Pola I, et al. Comparison of two plasma p-tau217 assays to detect and monitor Alzheimer's pathology. *EBioMedicine*. 2024;102:105046. [10.1016/j.ebiom.2024.105046](https://doi.org/10.1016/j.ebiom.2024.105046)
41. Braak H, Braak E. Neuropathological staging of Alzheimer-related changes. *Acta Neuropathol*. 1991;82(4):239-259. [10.1007/BF00308809](https://doi.org/10.1007/BF00308809)
42. Murray ME, Graff-Radford NR, Ross OA, Petersen RC, Duara R, Dickson DW. Neuropathologically defined subtypes of Alzheimer's

- disease with distinct clinical characteristics: a retrospective study. *Lancet Neurol.* 2011;10(9):785-96. [10.1016/S1474-4422\(11\)70156-9](https://doi.org/10.1016/S1474-4422(11)70156-9)
43. Whitwell JL, Dickson DW, Murray ME, et al. Neuroimaging correlates of pathologically defined subtypes of Alzheimer's disease: a case-control study. *Lancet Neurol.* 2012;11(10):868-877. [10.1016/S1474-4422\(12\)70200-4](https://doi.org/10.1016/S1474-4422(12)70200-4)
44. Ossenkoppele R, Rabinovici GD, Smith R, et al. Discriminative accuracy of [¹⁸F]flortaucipir positron emission tomography for Alzheimer disease vs other neurodegenerative disorders. *JAMA.* 2018;320(11):1151-1162. [10.1001/jama.2018.12917](https://doi.org/10.1001/jama.2018.12917)
45. Stanley K, Walker Z, Koopmans R, Rosness T. Do patients with young onset Alzheimer's disease deteriorate faster than those with late onset Alzheimer's disease? A review of the literature'. *Int Psychogeriatr.* 2014;26(12):1945-1953. [10.1017/S1041610214001173](https://doi.org/10.1017/S1041610214001173)
46. Panegyres PK, Chen HY. Differences between early and late onset Alzheimer's disease. *Am J Neurodegenerative Dis.* 2013;2(4).
47. Hwang J, Kim CM, Jeon S, et al. Prediction of Alzheimer's disease pathophysiology based on cortical thickness patterns. *Alzheimers Dement (Amst).* 2016;2:58-67. [10.1016/j.dadm.2015.11.008](https://doi.org/10.1016/j.dadm.2015.11.008)
48. Wennström M, Janelidze S, Nilsson KP, et al. Cellular localization of p-tau217 in brain and its association with p-tau217 plasma levels. *Acta Neuropathol Commun.* 2022;10(1). [10.1186/s40478-021-01307-2](https://doi.org/10.1186/s40478-021-01307-2)
49. Chen Q, Przybelski SA, Senjem ML, et al. Longitudinal tau positron emission tomography in dementia with Lewy bodies. *Mov Disord.* 2022;37(6):1256-1264. [10.1002/mds.28973](https://doi.org/10.1002/mds.28973)
50. Franzmeier N, Roemer-Cassiano SN, Bernhardt AM, et al. Alpha synuclein co-pathology is associated with accelerated amyloid-driven tau accumulation in Alzheimer's disease. *Mol Neurodegener.* 2025;20(1):31. [10.1186/s13024-025-00822-3](https://doi.org/10.1186/s13024-025-00822-3)

SUPPORTING INFORMATION

Additional supporting information can be found online in the Supporting Information section at the end of this article.

How to cite this article: Hojjati SH, Butler TA, Zare SJM, et al.; for the Alzheimer's Disease Neuroimaging Initiative. Diagnostic utility of plasma p-tau217 differs by Alzheimer's disease tau-based subtypes. *Alzheimer's Dement.* 2025;17:e70227. <https://doi.org/10.1002/dad2.70227>